

Anisotropy of the paramagnetic susceptibility in LaTiO₃: the electron-distribution picture in the ground state

R. M. Eremina, Mikhail V. Eremin, V. V. Iglamov, Joachim Hemberger,
Hans-Albrecht Krug von Nidda, Frank Lichtenberg, Alois Loidl

Angaben zur Veröffentlichung / Publication details:

Eremina, R. M., Mikhail V. Eremin, V. V. Iglamov, Joachim Hemberger, Hans-Albrecht Krug von Nidda, Frank Lichtenberg, and Alois Loidl. 2004. "Anisotropy of the paramagnetic susceptibility in LaTiO₃: the electron-distribution picture in the ground state." *Physical Review B* 70 (22): 224428. <https://doi.org/10.1103/PhysRevB.70.224428>.



Anisotropy of the paramagnetic susceptibility in LaTiO_3 : The electron-distribution picture in the ground state

R. M. Eremina,^{1,3} M. V. Eremin,^{2,3} V. V. Igiamov,² J. Hemberger,³ H.-A. Krug von Nidda,^{3,*} F. Lichtenberg,⁴ and A. Loidl³

¹*E. K. Zavoisky Physical Technical Institute, 420029 Kazan, Russia*

²*Kazan State University, 420008 Kazan, Russia*

³*Experimental Physics V, Electronic Correlations and Magnetism, Institute of Physics, University of Augsburg, 86135 Augsburg, Germany*

⁴*Experimental Physics VI, Electronic Correlations and Magnetism, Institute of Physics, University of Augsburg, 86135 Augsburg, Germany*

(Received 10 July 2004; published 22 December 2004)

The energy-level scheme and wave functions of the titanium ions in LaTiO_3 are calculated using crystal-field theory and spin-orbit coupling. The theoretically derived temperature dependence and anisotropy of the magnetic susceptibility agree well with experimental data obtained in an untwinned single crystal. The refined fitting procedure reveals an almost isotropic molecular field and a temperature dependence of the van Vleck susceptibility. The charge distribution of the $3d$ -electron on the Ti positions and the principle values of the quadrupole moments are derived and agree with NMR data and recent measurements of orbital momentum $\langle l \rangle$ and crystal-field splitting. The low value of the ordered moment in the antiferromagnetic phase is discussed.

DOI: 10.1103/PhysRevB.70.224428

PACS number(s): 75.30.Gw, 71.70.Ch, 71.30.+h, 71.27.+a

I. INTRODUCTION

In the physics of highly correlated electron systems the electronic orbitals and their interactions are in the focus of recent experimental and theoretical research, because the orbitals play a key role in the coupling of charge and spin of the electrons with the lattice. Transition-metal oxides, where the shape and anisotropy of the d -electron orbitals determine the fundamental electronic properties, provide a rich field for this kind of investigation. For example, the perovskite titanates ATiO_3 (with $A=\text{Y, La}$, or some trivalent rare-earth ion) are known as realization of a Mott insulator. The $3d^1$ electronic configuration of Ti^{3+} corresponds to an effectively half-filled conduction band, where the on-site Coulomb repulsion inhibits double occupation of the Ti sites resulting in an insulating ground state.¹ Although from their electronic configuration these titanates seem to be quite simple model systems, their orbital properties still have to be resolved especially in the case of LaTiO_3 .

The debate on the orbital ground state of LaTiO_3 was triggered by its unusual magnetic properties. Below the Néel temperature $T_N=146\text{ K}$,² LaTiO_3 reveals a slightly canted G -type antiferromagnetic structure with an ordered moment of $0.46\mu_B$,^{3,4} which is strongly reduced as compared to the spin-only value of $1\mu_B$ and, hence, indicates a strong importance of the spin-orbit coupling. On the other hand the nearly isotropic spin-wave dispersion with a small gap of about 3 meV contradicts a dominant spin-orbit coupling.⁵

This puzzling situation originates from the fact that the orthorhombic GdFeO_3 structure of LaTiO_3 deviates only weakly from the ideal cubic perovskite structure: The quasicubic crystal field of the nearly ideal oxygen octahedron surrounding the Ti^{3+} ion splits the five orbital $3d$ levels into a lower t_{2g} triplet and an excited e_g doublet. The single electron occupies the lower t_{2g} triplet and is Jahn-Teller active.⁶ In principle, the Jahn-Teller effect is expected to lift the re-

maining threefold degeneracy resulting in a distortion of the oxygen octahedron in favor of one of the three orbitals. However, the competing influence of spin-orbit coupling cannot be neglected in the case of a single electron in a t_{2g} level, as has been outlined already by Goodenough⁷ and by Kugel and Khomskii.⁸ It is important to note that, as long as the orbital triplet remains degenerate, the exchange interactions are inherently frustrated even in a cubic lattice.⁹

To promote possible physics of this degeneracy in LaTiO_3 , an orbital-liquid ground state has been suggested.¹⁰ Further detailed theoretical studies^{11,12} favoring the orbital-liquid image worked out that the frustration can be resolved via an order-by-disorder mechanism giving rise to magnetic spin order with disordered orbital states. The observed spin-wave excitations were found to be in accord with this model. However it is necessary to mention that a recent analysis has shown that the Kugel-Khomskii Hamiltonian taken in strictly cubic symmetry does not support any long-range magnetic order at all (Harris *et al.*¹³) and, therefore, the authors have questioned this model as an appropriate starting point to describe LaTiO_3 . In a different theoretical approach^{14–18} the crystal field of the La ions caused by the GdFeO_3 -type distortion has been shown to lift the degeneracy of the $\text{Ti-}t_{2g}$ -orbitals and to stabilize the antiferromagnetic G -type order. In Refs. 14–16 the orbital-ground state was derived as approximately $3z_{11}^2 - r^2 = (d_{xy} + d_{yz} + d_{zx})/\sqrt{3}$. However, Solovyev¹⁸ has found that the Hartree-Fock approximation alone fails to provide the description of the magnetic properties of LaTiO_3 and YTiO_3 .

Several recent experimental investigations strongly support the existence of orbital order in LaTiO_3 . Specific-heat, electrical resistivity, thermal-expansion, and infrared experiments¹⁹ exhibit anomalies near the Néel temperature, which indicate significant structural changes and have been interpreted in terms of the influence of orbital order via magnetoelastic interactions. Transmission-electron microscopy

revealed small atomic displacements ascribed to a weak Jahn-Teller distortion.²⁰ Detailed x-ray and neutron-diffraction studies²¹ of crystal and magnetic structure revealed an intrinsic distortion of the oxygen octahedra, which leads to a large enough splitting of the Ti- t_{2g} triplet state. The remeasured magnetic moment $\mu=0.57(5)\mu_B$ turned out to be slightly larger than already determined.²¹ The reexamination of the Ti nuclear magnetic resonance spectra²² proves a large nuclear quadrupole splitting, which is ascribed to a rather large quadrupole moment of the 3d electrons at the Ti sites. This discarded the earlier interpretation²³ of the NMR results in terms of orbital degeneracy and clearly favored the orbital order.

In this article we perform a detailed analysis of the temperature dependence and anisotropy of the magnetic susceptibility of LaTiO₃, which we obtained on an untwinned single crystal. In an earlier publication²⁴ it was mentioned that the anisotropy observed in the paramagnetic regime is required to include the spin-orbit coupling into the crystal-field calculation. In the present analysis we develop this approach and go beyond the Hartree-Fock approximation.¹⁸ Besides the spin-orbit coupling we are taking into account the Ti-O exchange as well. We will show that the obtained orbital-order pattern is basically in agreement with NMR data²² and describes consistently the temperature dependence and anisotropy of the observed experimental susceptibility.

II. CRYSTAL FIELD ANALYSIS

In LaTiO₃ the Ti³⁺ ions (electronic configuration 3d¹, spin $s=1/2$) are situated in slightly distorted octahedra formed by the oxygen ions. The dominant cubic component of the crystal field splits the five 3d-electron states into a lower triplet t_{2g} and an upper doublet e_g . The low-symmetry component of the crystal field is expected to be small with respect to the cubic one and, therefore, one may be tempted to analyze the magnetic susceptibility using the basis of the t_{2g} states with a fictitious orbital momentum $\tilde{l}=1$.²⁵ However, this procedure is not convenient for LaTiO₃ for the following reason. The wave functions of the fictitious momentum $\tilde{l}=1$ are defined in a local coordinate system (x, y, z) with its axes parallel to the C_4 axes of the nondistorted octahedra. In the real structure of LaTiO₃, there are four different fragments TiO₆, which are distorted and rotated with respect to each other, i.e., the $\tilde{l}=1$ basis should be rotated correspondingly for each of the four inequivalent octahedra. During these rotations all 3d-electron states are mixed. In this situation it is preferable to stay in the crystallographic coordinate system using the full basis of 3d-electron states.

Thus, to determine the energy-level scheme of Ti³⁺ in LaTiO₃, we start from the Hamiltonian:

$$\mathcal{H}_0 = \xi(\mathbf{l}\mathbf{s}) + \sum_{k=2,4} \sum_{q=-k}^k B_q^{(k)} C_q^{(k)}(\vartheta, \varphi). \quad (1)$$

The first term denotes the spin-orbit coupling with spin \mathbf{s} and orbital momentum \mathbf{l} . For Ti³⁺ the parameter of the spin-orbit coupling is expected to be about $\xi \approx 200$ K.²⁵ The second

term represents the crystal field with the spherical tensor $C_q^{(k)}(\vartheta, \varphi) = \sqrt{2\pi/(2k+1)} Y_q^{(k)}(\vartheta, \varphi)$. The crystal-field parameters

$$B_q^{(k)} = \sum_j a^{(k)}(R_j) (-1)^q C_{-q}^{(k)}(\vartheta_j, \varphi_j) \quad (2)$$

are calculated using available data about the crystal structure.^{26–28} The sum runs over the lattice sites R_j .

The main contributions to the quantities $B_q^{(k)}$ originate from the point charges Z_j of the lattice and so-called exchange charges. Hence, the intrinsic parameters of the crystal field are given by

$$a^{(k)}(R_j) = -\frac{Z_j e^2 \langle r^k \rangle}{R_j^{k+1}} + a_{\text{ex}}^{(k)}(R_j). \quad (3)$$

The exchange contribution originates from the charge transfer from oxygen into the unfilled 3d shell, i.e., the covalence effect, and the direct titanium-oxygen exchange coupling.^{29,30}

$$a_{\text{ex}}^{(2)}(R_j) = \frac{G}{R_j} (S_{3d\sigma}^2 + S_{3ds}^2 + S_{3d\pi}^2) \\ a_{\text{ex}}^{(4)}(R_j) = \frac{9G}{5R_j} \left(S_{3d\sigma}^2 + S_{3ds}^2 - \frac{4}{3} S_{3d\pi}^2 \right), \quad (4)$$

where $S_{3d\sigma}$, $S_{3d\pi}$, and S_{3ds} denote the overlap integrals for Ti³⁺(3d¹)-O²⁻(2s²2p⁶), which are determined in local coordinate systems with the z axis along the titanium-oxygen bond. All integrals are calculated using the Hartree-Fock wave functions³¹ of Ti³⁺ and O²⁻. The parameter $G=7.2$ is an adjustable parameter, which we have extracted from the cubic crystal-field splitting parameter $10Dq$, which can be assumed as approximately similar for all titanium oxides as, e.g., for Ti³⁺ in Al₂O₃ with $10Dq=19\,000$ cm⁻¹.²⁵

In LaTiO₃ there is no inversion symmetry at the oxygen position and, therefore, each oxygen ion exhibits a dipole moment $\mathbf{d}_i = \alpha \mathbf{E}_i$, where α denotes the polarization constant³² and \mathbf{E}_i is the electric field of the surrounding ions at the oxygen site with number i . For the oxygen positions^{27,28} O₁($X=0.490\,36$, 0.25 , $Z=0.078\,13$) and O₂($x=0.291\,44$, $y=0.041\,16$, $z=0.710\,36$) at $T=298$ K, the values of the dipole moments (in units of $e\text{\AA}$) were calculated as $d_x=-0.093$, $d_y=0$, $d_z=-0.001$ (O₁), and $d_x=0.036$, $d_y=0.018$, $d_z=0.037$ (O₂), respectively. The relative signs for the other three O₁ and seven O₂ positions change like the signs of the corresponding coordinates (X , Z , and x , y , z), e.g., for the O₁ position ($X+0.5$, 0.25 , and $0.5-Z$) we obtain $d_x=-0.093$, $d_y=0$, $d_z=0.001$, etc. The corresponding expressions for corrections to the crystal-field parameters $B_0^{(2)}$, $B_2^{(2)}$, and $B_4^{(2)}$ are calculated as usual.³²

In the crystallographic coordinate system, with the Cartesian axes x , y , and z chosen along the crystal axes $a=5.6071$ Å, $b=7.9175$ Å, and $c=5.6247$ Å in $Pnma$ representation (corresponding to b , c , and a in $Pbnm$ representation, which is used in many papers), respectively (values at room temperature 298 K) we obtain the crystal-field parameters (in K) for the titanium ion in position Ti₁($\frac{1}{2}, \frac{1}{2}, 0$) as

TABLE I. Contributions to the crystal-field parameters in LaTiO₃ at the Ti₁ position ($\frac{1}{2}, \frac{1}{2}, 0$) in units of K.

$B_q^{(k)}$	Point charges	Exchange charges	Dipolar
$B_0^{(2)}$	1527	720	-819
$B_1^{(2)}$	-162- <i>i</i> 376	-301+ <i>i</i> 62	1548- <i>i</i> 413
$B_2^{(2)}$	-1229+ <i>i</i> 2496	-941+ <i>i</i> 103	430+ <i>i</i> 1525
$B_0^{(4)}$	-4486	-7713	small
$B_1^{(4)}$	-5828+ <i>i</i> 4105	10951+ <i>i</i> 7733	small
$B_2^{(4)}$	11325- <i>i</i> 1699	19452- <i>i</i> 2160	small
$B_3^{(4)}$	1827+ <i>i</i> 7634	3407+ <i>i</i> 14371	small
$B_4^{(4)}$	7638+ <i>i</i> 1713	13047+ <i>i</i> 2963	small

given in Table I. For the other three titanium positions the absolute values of $B_q^{(k)}$ are the same, but their signs are different (cf. Table II). Note that the quantum mechanical contributions are comparable to the classical ones and even dominate for $k=4$.

Using the crystal-field parameters listed above, for the position Ti₁($\frac{1}{2}, \frac{1}{2}, 0$) we obtain the following energy spectrum of five Kramers doublets with energies $\varepsilon_{1,2}/k_B=0$, $\varepsilon_{3,4}/k_B=2553$ K, $\varepsilon_{5,6}/k_B=3214$ K, $\varepsilon_{7,8}/k_B=26\,773$ K, and $\varepsilon_{9,10}/k_B=27\,890$ K. This excitation spectrum agrees perfectly with results from FIR experiments, which reveal a hump in the optical conductivity close to 3000 K.³³ It is also in good agreement with the results of recent spin-polarized photoelectron spectroscopy experiments, which yield a crystal-field splitting of 0.12–0.30 eV, i.e., 1300–3300 K, of the t_{2g} subshell.³⁴ The corresponding wave functions in $|m_l, m_s\rangle$ quantization are written as follows:

$$|\varepsilon_n\rangle = \sum_{m_l=-2}^{+2} \sum_{m_s=\uparrow, \downarrow} a_{m_l, m_s}^{(n)} |m_l, m_s\rangle. \quad (5)$$

In particular for one of the components of the ground doublet of Ti₁($\frac{1}{2}, \frac{1}{2}, 0$) the coefficients are explicitly given in Table III. The other component of the ground state can be obtained as Kramers conjugated state. Note that the g -values $g_z=2\langle\varepsilon_1|k_z I_z+2s_z|\varepsilon_1\rangle$, $g_x=2\langle\varepsilon_1|k_x I_x+2s_x|\varepsilon_2\rangle$, and $g_y=2\langle\varepsilon_1|k_y I_y+2s_y|\varepsilon_2\rangle$ are equal for all four titanium posi-

TABLE II. Relative signs of the parameters $B_q^{(k)}$ for Ti₂, Ti₃, and Ti₄ with respect to the signs for the Ti₁ position in LaTiO₃.

	Ti2($0, \frac{1}{2}, \frac{1}{2}$)	Ti3($\frac{1}{2}, 0, 0$)	Ti4($0, 0, \frac{1}{2}$)
$B_0^{(2)}$	+	+	+
$B_1^{(2)}$	Re-, Im-	Re+, Im-	Re-, Im+
$B_2^{(2)}$	Re+, Im+	Re+, Im-	Re+, Im-
$B_0^{(4)}$	+	+	+
$B_1^{(4)}$	Re-, Im-	Re+, Im-	Re-, Im+
$B_2^{(4)}$	Re+, Im+	Re+, Im-	Re+, Im-
$B_3^{(4)}$	Re-, Im-	Re+, Im-	Re-, Im+
$B_4^{(4)}$	Re+, Im+	Re+, Im-	Re+, Im-

TABLE III. Coefficients of the ground-state wave functions in LaTiO₃ at the Ti₁ position ($\frac{1}{2}, \frac{1}{2}, 0$).

$a_{m_l, m_s}^{(1)}$	$m_s=\uparrow$	$m_s=\downarrow$
$m_l=2$	-0.479- <i>i</i> 0.191	-0.033- <i>i</i> 0.031
$m_l=1$	0.136+ <i>i</i> 0.025	0.005- <i>i</i> 0.020
$m_l=0$	-0.032+ <i>i</i> 0.608	-0.011+ <i>i</i> 0.030
$m_l=-1$	0.154- <i>i</i> 0.047	-0.012- <i>i</i> 0.007
$m_l=-2$	0.526- <i>i</i> 0.186	0.048

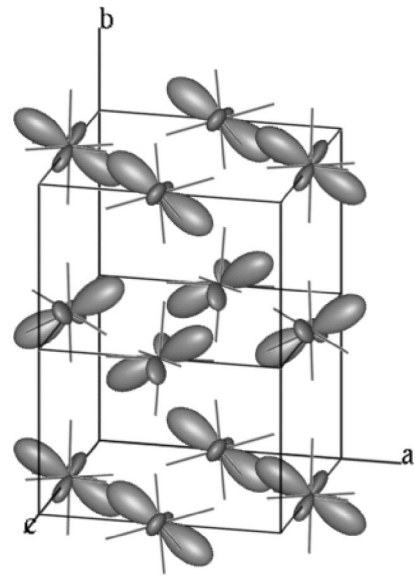
tions, i.e., $g_z=1.81$, $g_x=1.73$, $g_y=1.79$, where the reduction factors of the orbital momentum due to covalency have been assumed as $k_\alpha=1$. The relatively small deviation of the g value from the spin-only value 2 displays that the orbital momentum is rather small, again in agreement with the recent spin-resolved photoemission experiments.³⁴

Figure 1 illustrates the orbital order pattern due to the derived ground-state wave function (cf. Table III). Basically, this is in agreement with the order patterns found by Cwik *et al.*,²¹ by Kiyama and Itoh,²² and by Pavarini *et al.*¹⁶ However, in those works the wave functions have been approximated in terms of the $t_{2g}^{(111)}$ basis only, neglecting the spin-orbit coupling.

Having obtained the orbital ground state, we are able to determine the charge distribution at the Ti sites characterized by the quadrupole moments. The tensor of the quadrupole moment per one Ti position is given by

$$Q_{\alpha\beta} = \frac{2}{21} |e|\langle r^2 \rangle \langle 3I_\alpha I_\beta - 6\delta_{\alpha\beta} \rangle. \quad (6)$$

Diagonalization of the tensors $Q_{\alpha\beta}/(|e|\langle r^2 \rangle)$ calculated for all four Ti positions yields the same principal values equal to $Q_1=-0.520$, $Q_2=0.460$, and $Q_3=0.060$, i.e., the charge dis-

FIG. 1. Orbital order in LaTiO₃ as derived from the crystal-field analysis.

tribution on the titanium ions is the same in the local coordinate systems, which are rotated with respect to each other. The angles of rotations have been calculated via the eigenvectors of the tensors $Q_{\alpha\beta}$. The components of the unit vectors (n_x , n_y , and n_z) corresponding to the principal values -0.520 and 0.460 read $\mathbf{n}_1 = (0.815, 0.573, \text{ and } 0.086)$ and $\mathbf{n}_2 = (-0.573, 0.746, \text{ and } 0.355)$ at the Ti_1 site. For -0.520 (0.460) n_y (n_x) is reversed at the Ti_3 and Ti_4 sites, whereas n_z is reversed at the Ti_2 (Ti_2) and Ti_4 (Ti_3) sites.

It is interesting to know, how the spin is oriented with respect to the quadrupole charge distribution. According to neutron-scattering data^{21,35} and susceptibility measurements^{4,24} the effective magnetic moment per one Ti^{3+} is about $\mu_{\text{eff}} \sim 0.6\mu_B$. The antiferromagnetically ordered moments are aligned along the c direction and weak ferromagnetism shows up along the b direction (in $Pnma$).²¹ We suggest that this can be explained as follows. Due to the spin-orbit coupling the orientations of the titanium magnetic moments are connected with the quadrupole ordering. If we assume that the spin is aligned perpendicular to the $3d$ -electron charge-distribution plane, i.e., along \mathbf{n}_2 , a ferromagnetic alignment along the b axis can result from the y component of \mathbf{n}_2 , which is positive at all four Ti places, and a G -type antiferromagnetic order along the c axis is favored as the sign of the z component of \mathbf{n}_2 changes between the Ti sites, correspondingly. As neutron scattering detects the averaged magnetic moment of the four inequivalent Ti places per unit cell with vice versa twisting of the quadrupolar moments, the observed $\mu_{\text{eff}} \sim 0.6\mu_B$ is just the projection of the total magnetic moments onto the c direction.

III. MAGNETIC SUSCEPTIBILITY

The LaTiO_3 single crystal, prepared by floating zone melting,² was essentially the same as used previously for the thermal-expansion measurements described in Ref. 19. The crystallographic axes were determined from x-ray Laue pictures. Additional neutron-diffraction experiments³⁵ on the same crystal revealed only a small twin domain of about 5% of the crystal volume, hence the crystal can be regarded as practically untwinned. The magnetization $M(T)$ was measured in a commercial superconducting quantum interference device (SQUID) magnetometer (MPMS5, Quantum Design), working in a temperature range $1.8 \leq T \leq 400$ K and in magnetic fields up to $H = 50$ kOe.

Figure 2 shows the temperature dependence of the susceptibility $\chi = M/H$ obtained from the LaTiO_3 single crystal in an external field of $H = 10$ kOe applied along the three orthorhombic axes both below T_N (inset) and in inverse representation in the paramagnetic regime (main frame). The data have been corrected accounting for the diamagnetic background of the sample holder, which was measured independently for all three geometries. Below the Néel temperature $T_N = 146$ K, one observes the evolution of a weak ferromagnetic magnetization of about $0.02\mu_B$ per formula unit with its easy direction along the b axis. The paramagnetic regime is better visible in the inverse susceptibility with an approximately linear increase above 200 K. Evaluation by a Curie-Weiss behavior $N_A\mu_{\text{eff}}^2/3k_B(T + \Theta_{\text{CW}})$, with $\mu_{\text{eff}}^2 = \mu_B^2 S(S$

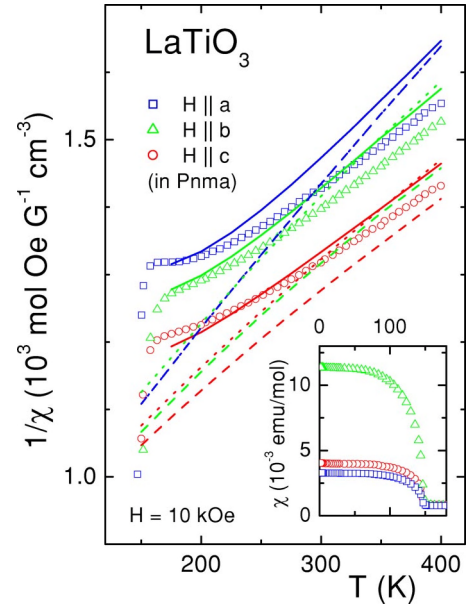


FIG. 2. (Color online) Temperature dependence of the inverse susceptibility $1/\chi(T)$ [inset: $\chi(T)$ at low temperatures] in LaTiO_3 for an external field of $H = 10$ kOe applied along the three crystallographic axes a , b , and c ($Pnma$). The fits indicated by solid, dashed, and dotted lines are described.

+1) yields a Curie-Weiss temperature $\Theta_{\text{CW}} \approx 900$ K and an effective moment $\mu_{\text{eff}} \approx 2.6\mu_B$, which is strongly enhanced with respect to the spin-only value of $1.73\mu_B$. For an appropriate evaluation we have to take into account the preceding energy-level scheme derived from our CF analysis.

Including the external magnetic field, the perturbation Hamiltonian is written as

$$V = -\mu_B H_\alpha (k_\alpha J_\alpha + 2s_\alpha - f_\alpha s_\alpha) = -H_\alpha M_\alpha, \quad (7)$$

where the factors f_α take into account the molecular field, which can be anisotropic for two reasons. The first one is because of the anisotropic g factors. The second one is due to the anisotropy of the effective superexchange interaction between the titanium spins, which we take in the form $\sum_\alpha J_{ij}^\alpha s_i^\alpha s_j^\alpha$. The parameters J_{ij}^α represent the effective superexchange integrals, $\alpha = x, y, \text{ and } z$. In the crystal structure around each Ti^{3+} ion, there are two titanium ions at a distance $R_1 = 3.958$ Å, four titanium ions at $R_2 = 3.971$ Å, and 12 at a distance $R_3 = 5.6$ Å. According to the neutron-scattering data⁵ $J_1^\alpha \approx J_2^\alpha \approx 180$ K for all α .

The molecular field approximation taking into account the six nearest neighbors at distances R_1 and R_2 yields

$$f_\alpha = \frac{6J_\alpha \langle s_\alpha \rangle \langle k_\alpha J_\alpha + 2s_\alpha \rangle}{k_B T + 6J_\alpha \langle s_\alpha \rangle^2} = \frac{C_\alpha}{T + \Theta_\alpha}. \quad (8)$$

Note, that in this approximation the ratios C_α/Θ_α are independent on the exchange coupling J_α and directly determined by the spin and orbital state as

$$\frac{C_\alpha}{\Theta_\alpha} = \frac{\langle \varepsilon_1 | k_\alpha J_\alpha + 2s_\alpha | \varepsilon_1 \rangle}{\langle \varepsilon_1 | s_\alpha | \varepsilon_1 \rangle}. \quad (9)$$

The ratios $C_x/\Theta_x \approx 1.92$ and $C_y/\Theta_y \approx 1.85$, and $C_z/\Theta_z \approx 1.80$, as calculated from the ground state assuming $k_\alpha = 1$, indicate again a small contribution of the orbital momentum l_α to the magnetic susceptibility. For zero orbital momentum one would obtain $C_\alpha/\Theta_\alpha = 2$.

For $\alpha = z$ the paramagnetic part of the susceptibility can be written as

$$\chi_{\text{para}}^{zz} = \frac{1}{Z} \sum_l \langle \varepsilon_l | M_z | \varepsilon_l \rangle^2 \exp(-\varepsilon_l/k_B T), \quad (10)$$

where $Z = k_B T \sum_l \exp(-\varepsilon_l/k_B T)$. The van Vleck like contribution reads

$$\chi_{vv}^{zz} = 2 \sum_l \frac{\langle \varepsilon_1 | M_z | \varepsilon_l \rangle \langle \varepsilon_l | M_z | \varepsilon_1 \rangle}{\varepsilon_l - \varepsilon_1}. \quad (11)$$

The cases $\alpha = x, y$ can be written analogously. In addition, one has to take into account the diamagnetic susceptibility. It can be estimated from the ionic susceptibilities³⁶ (given in 10^{-6} emu/mol) of La^{3+} (-20), Ti^{3+} (-9), and O^{2-} (-12) as $\chi_{\text{dia}} = -6.5 \times 10^{-5}$ emu/mol.

In Fig. 2 the theoretical description of the data has been performed in three steps, as illustrated by the three groups of dashed, dotted, and solid lines, respectively. In the first step (dashed lines) the exchange coupling is assumed to be isotropic and used as the only fit parameter $J_\alpha = J$. The reduction factors have been kept fixed at $k_\alpha = 1$. With $J = 200$ K in good agreement with the results of neutron scattering, one achieves a reasonable description of the susceptibility. It is remarkable that absolute value and anisotropy are very well reproduced by this straightforward calculation.

In the second step, we allowed a variation of the covalency parameters k_α . With the same exchange constant of 200 K and $k_x = 1$, $k_y = 0.88$, and $k_z = 0.95$ (dotted lines) the description of the relative splitting of the susceptibilities between the different axes is improved, but the curvature is still not reproduced. Nevertheless, the obtained covalency parameters match the values typically observed for Ti^{3+} ions.²⁵ The resulting ratios C_α/Θ_α change only slightly $C_x/\Theta_x \approx 1.92$ and $C_y/\Theta_y \approx 1.87$, and $C_z/\Theta_z \approx 1.81$ with respect to $k_\alpha = 1$.

Finally in the third step, the solid lines show the fit of the experimental data using in addition the values C_α and Θ_α as adjustable parameters. From fitting we have got C_x/Θ_x

$= 2.45$, $C_y/\Theta_y = 2.29$, and $C_z/\Theta_z = 2.14$. These deviations from the nearest-neighbor isotropic molecular-field results can be considered as a hint for a spin-orbit dependent exchange like $J(s_i s_j) l_\alpha^i l_\beta^j$ between the titanium ions. In principle, operators such as these are known and have been discussed in a number of papers³⁷⁻⁴⁰ in application to the susceptibility of the dimer $[\text{Ti}_2\text{Cl}_9]^{-3}$ and *a priori* cannot be discarded for LaTiO_3 . Another influence, which in our opinion cannot be excluded, is the next nearest neighbor interaction between the titanium ions. Obviously this question should be addressed to further analysis, when more experimental information will be obtained. However, both types of interactions mentioned can produce the corrections of a few percent, but we believe that the essential physics of the temperature dependence of magnetic susceptibility and orbital ordering will be the same as described above.

Note that the factor f_α is quite large and, therefore, according to Eq. (11) $\chi_{vv}^{\alpha\alpha}$ is dependent on temperature. This fact has not been pointed out in literature. We think that this situation should be quite general for other titanium compounds as well as for vanadium oxides.

IV. CONCLUSIONS

In summary the energy splitting and wave functions of the Ti^{3+} $3d^1$ -electron state have been calculated for LaTiO_3 due to the crystal field including spin-orbit coupling and Ti-O exchange. From the derived orbital ground state we have estimated the quadrupole moments at the Ti sites and have deduced the charge-distribution image for the $3d$ electrons in the crystallographic coordinate system. Based on the orientation of the quadrupolar tensor, it is possible to suggest an explanation for the low value of the ordered moment, observed in the antiferromagnetic state. The straightforward calculation of the paramagnetic susceptibility yields the correct anisotropy, which we measured in an untwinned LaTiO_3 single crystal.

ACKNOWLEDGMENTS

The authors thank Dana Vieweg for performing the SQUID measurements. This work is supported by the German Bundesministerium für Bildung und Forschung (BMBF) under Contract No. VDI/EKM 13N6917, by the Deutsche Forschungsgemeinschaft (DFG) via Sonderforschungsbereich SFB 484 (Augsburg), by the Russian RFFI (Grant No. 03 02 17430), and partially by CRDF (BRHE REC007).

*Electronic address: hans-albrecht.krug@physik.uni-augsburg.de

¹Y. Okimoto, T. Katsufuji, Y. Okada, T. Arima, and Y. Tokura, Phys. Rev. B **51**, 9581 (1995).

²F. Lichtenberg, D. Widmer, J. G. Bednorz, T. Williams, and A. Reller, Z. Phys. B: Condens. Matter **82**, 211 (1991).

³J. P. Goral and J. E. Greedan, J. Magn. Magn. Mater. **37**, 315 (1983).

⁴G. I. Meijer, W. Henggeler, J. Brown, O.-S. Becker, J. G. Bednorz, and C. Rossel, and P. Wachter, Phys. Rev. B **59**, 11 832 (1999).

⁵B. Keimer, D. Casa, A. Ivanov, J. W. Lynn, M. v. Zimmermann, J. P. Hill, D. Gibbs, Y. Taguchi, and Y. Tokura, Phys. Rev. Lett. **85**, 3946 (2000).

⁶H.-A. Jahn and E. Teller, Proc. R. Soc. London, Ser. A **161**, 220

- (1937).
- ⁷J. B. Goodenough, Phys. Rev. **171**, 466 (1968).
 - ⁸K. I. Kugel and D. Khomskii, Sov. Phys. Usp. **25**, 231 (1982).
 - ⁹D. I. Khomskii and M. V. Mostovoy, J. Phys. A **36**, 9197 (2003).
 - ¹⁰G. Khaliullin and S. Maekawa, Phys. Rev. Lett. **85**, 3950 (2000).
 - ¹¹G. Khaliullin, Phys. Rev. B **64**, 212405 (2001).
 - ¹²K. Kikoin, O. Entin-Wohlman, V. Fleurov, and A. Aharony, Phys. Rev. B **67**, 214418 (2003).
 - ¹³A. B. Harris, A. Aharony, O. Entin-Wohlman, I. Ya.Korenblit, and T. Yildirim, Phys. Rev. B **69**, 094409 (2004); A. B. Harris, T. Yildirim, A. Aharony, O. Entin-Wohlman, and I. Ya.Korenblit, Phys. Rev. Lett. **91**, 087206 (2003).
 - ¹⁴M. Mochizuki and M. Imada, J. Phys. Soc. Jpn. **70**, 2872 (2001).
 - ¹⁵M. Mochizuki and M. Imada, Phys. Rev. Lett. **91**, 167203 (2003).
 - ¹⁶E. Pavarini, S. Biermann, A. Poteryaev, A. I. Lichtenstein, A. Georges, and O. K. Andersen, Phys. Rev. Lett. **92**, 176403 (2004).
 - ¹⁷L. Craco, M. S. Laad, S. Leoni, and E. Müller-Hartmann, cond-mat/0309370 (2003).
 - ¹⁸I. V. Solovyev, Phys. Rev. B **69**, 134403 (2004).
 - ¹⁹J. Hemberger, H.-A. Krug von Nidda, V. Fritsch, J. Deisenhofer, S. Lobina, T. Rudolf, P. Lunkenheimer, F. Lichtenberg, A. Loidl, D. Bruns, and B. Büchner, Phys. Rev. Lett. **91**, 066403 (2003).
 - ²⁰M. Arao, Y. Inoue, and Y. Koyama, J. Phys. Chem. Solids **63**, 995 (2002).
 - ²¹M. Cwik, T. Lorenz, J. Baier, R. Müller, G. André, F. Bourée, F. Lichtenberg, A. Freimuth, R. Schmitz, E. Müller-Hartmann, and M. Braden, Phys. Rev. B **68**, 060401(R) (2003).
 - ²²T. Kiyama and M. Itoh, Phys. Rev. Lett. **91**, 167202 (2003).
 - ²³M. Itoh, M. Tsuchiya, H. Tanaka, and K. Motoya, J. Phys. Soc. Jpn. **68**, 2783 (1999).
 - ²⁴V. Fritsch, J. Hemberger, M. V. Eremin, H.-A. Krug von Nidda, F. Lichtenberg, R. Wehn, and A. Loidl, Phys. Rev. B **65**, 212405 (2002).
 - ²⁵A. Abragam and B. Bleaney, *Electron Paramagnetic Resonance of Transition Ions* (Oxford University Press, London, 1971).
 - ²⁶*International Table for Crystallography*, edited by T. Hahn (Kluwer, Dordrecht, 1996), Vol. A, p. 289.
 - ²⁷D. A. MacLean, H. N. Ng, and J. E. Greedan, J. Solid State Chem. **30**, 35 (1979).
 - ²⁸M. Eitel and J. E. Greedan, J. Less-Common Met. **116**, 95 (1986).
 - ²⁹B. Z. Malkin, in *Spectroscopy of Solids Containing Rare-Earth Ions*, edited by A. A. Kaplyanskii and R. M. Macfarlane (Elsevier Science, Amsterdam, 1987), p. 13.
 - ³⁰M. V. Eremin and A. A. Kornienko, Phys. Status Solidi B **79**, 775 (1977); M. V. Eremin, Sov. Phys. Opt. Spectrosc. **68**, 860 (1990).
 - ³¹E. Clementi and A. D. McLean, Phys. Rev. A **133**, 419 (1964); E. Clementi and C. Roetti, At. Data Nucl. Data Tables **14**, 177 (1974).
 - ³²M. Faucher and D. Garcia, Phys. Rev. B **26**, 5451 (1982); G. D. Mahan, Solid State Commun. **33**, 797 (1980).
 - ³³P. Lunkenheimer, T. Rudolf, J. Hemberger, A. Pimenov, S. Tachos, F. Lichtenberg, and A. Loidl, Phys. Rev. B **68**, 245108 (2003).
 - ³⁴M. W. Haverkort, Z. Hu, A. Tanaka, G. Ghiringhelli, H. Roth, M. Cwik, T. Lorenz, C. Schüßler-Langeheine, S. V. Streltsov, A. S. Mylnikova, V. I. Anisimov, C. de Nadai, N. B. Brookes, H. H. Hsieh, H. J. Lin, C. T. Chen, T. Mizokawa, Y. Taguchi, Y. Tokura, D. I. Khomskii, and L. H. Tjeng, cond-mat/0405516 (2004).
 - ³⁵M. Reehuis (private communication).
 - ³⁶Landolt-Börnstein, New Series, Group II (Springer, Berlin, 1976), Vol. 8, Part 1, 27. As La^{3+} is not given in the tables, its value (-20) has been extrapolated from isoelectronic Cs^+ (-31) and Ba^{2+} (-24), comparing the series Rb^+ (-20), Sr^{2+} (-15), and Y^{3+} (-12).
 - ³⁷M. Drillon and R. Georges, Phys. Rev. B **26**, 3882 (1982).
 - ³⁸B. Leuenberger and H. U. Gudel, Mol. Phys. **51**, 1 (1984).
 - ³⁹Y. V. Rakitin, M. V. Eremin, and V. T. Kalinnikov, Koord. Khim. **21**, 200 (1995).
 - ⁴⁰J. J. Borrás-Almenar, J. M. Clemente-Juan, E. Coronado, A. Pali, and B. S. Tsukerblat, J. Chem. Phys. **114**, 1148 (2001).